



Region-specific associations among tissue-level mechanical properties, porosity, and composition in human male femora

Gurjit S. Mandair^a, Erin M.R. Bigelow^b, Gowri Viswanathan^a, Ferrous S. Ward^{b,c}, Daniella M. Patton^{b,c}, Stephen H. Schlecht^{b,d}, Karl J. Jepsen^{b,c}, David H. Kohn^{a,c,*}

^a Biological and Material Sciences, School of Dentistry, University of Michigan, Ann Arbor, MI, USA

^b Department of Orthopaedic Surgery, University of Michigan, Ann Arbor, MI, USA

^c Biomedical Engineering, University of Michigan, Ann Arbor, MI, USA

^d Mechanical Engineering, University of Michigan, Ann Arbor, MI, USA

ARTICLE INFO

Keywords:

Bone
Biomechanics
Aging
Men
Femora
Porosity
Composition

ABSTRACT

Region-specific differences in age-related bone remodeling are known to exist. We therefore hypothesized that the decline in tissue-level strength and post-yield strain (PYS) with age is not uniform within the femur, but is driven by region-specific differences in porosity and composition. Four-point bending was conducted on anterior, posterior, medial, and lateral beams from male cadaveric femora ($n = 33$, 18–89 yrs of age). Mid-cortical porosity, composition, and mineralization were assessed using nano-computed tomography (nanoCT), Raman spectroscopy, and ashing assays. Traits between bones from young and elderly groups were compared, while multivariate analyses were used to identify traits that predicted strength and PYS at the regional level. We show that age-related decline in porosity and mechanical properties varied regionally, with highest positive slope of age vs. Log(porosity) found in posterior and anterior bone, and steepest negative slopes of age vs. strength and age vs. PYS found in anterior bone. Multivariate analyses show that Log(porosity) and/or Raman 1246/1269 ratio explained 46–51% of the variance in strength in anterior and posterior bone. Three out of five traits related to Log(porosity), mineral crystallinity, 1246/1269, mineral/matrix ratio, and/or hydroxyproline/proline (Hyp/Pro) ratio, explained 35–50% of the variance in PYS in anterior, posterior and lateral bones. Log(porosity) and Hyp/Pro ratio alone explained 13% and 19% of the variance in strength and PYS in medial bone, respectively. The predictive performance of multivariate analyses was negatively impacted by pooling data across all bone regions, underscoring the complexity of the femur and that the use of pooled analyses may obscure underlying region-specific differences.

1. Introduction

Bone strength in midlife and older adults is contingent on accrual of bone mass during late childhood through early adolescence and subsequent loss of bone mass following peak accrual (Rizzoli et al., 2010). Bone strength is also derived from material properties. Material properties, in turn, are a function of porosity, which increases with age from 4 to 5% in young adults to ~11% by the eighth decade (Bell et al., 2001), and is mediated through intracortical remodeling (Goldman et al., 2014; Jepsen et al., 2011; Zebaze et al., 2019). Small increases in porosity can disproportionately reduce bone strength (Ramchand and Seeman, 2018; Turner, 2002) and fracture toughness (Granke et al., 2016; Yeni et al., 1997). Porosity may have clinical relevance in explaining the variance

in bone strength not captured by DXA (Choksi et al., 2018). Porosity changes in human femora can contribute ~76% of the variance in age-related decline in ultimate tensile stress, with a steeper decline in women than in men (McCalden et al., 1993).

Bone adapts to its local mechanical loading environment (Ruff et al., 2006), thus age-related changes in tissue mechanics or porosity are expected to be bone or region-specific. Human tibiae and femora exhibit differential age-related decline in ultimate tensile strain of 5 and 7% per decade, respectively (Burstein et al., 1976). Regional porosity differences in human femora have also been reported, with posterior bone exhibiting the highest porosity (Malo et al., 2013; Thomas et al., 2005). Regional porosity differences may reflect regional differences in the magnitude and mode of strain (Skedros et al., 2013). Osteons and

* Corresponding author at: Departments of Biologic and Materials Sciences and Biomedical Engineering, University of Michigan, Ann Arbor, MI, USA.

E-mail address: dhkohn@umich.edu (D.H. Kohn).

Haversian canal diameters (related to porosity) become smaller and osteon density larger in regions of high strain (Schlecht et al., 2012; Skedros et al., 2013; van Oers et al., 2008). Other studies report regional differences in the amount of diffuse microcracking and microdamage density, with anterior bone exhibiting more diffuse microcracking than posterior bone under compression (Reilly et al., 1999), and highest age-related microdamage density in anterior bone (Norman et al., 1997).

While correlations between select cortical bone composition parameters and age or mechanics have been studied for specific regions across the male femora (Yerramshetty and Akkus, 2008; Yerramshetty et al., 2006), comprehensive comparison of multiple human femoral bone traits related to porosity, composition, and tissue-level mechanical properties by region and age, and analysis of traits predictive of regional declines in strength and ductility with age have yet to be performed. Identifying regional predictors of tissue-level strength and post-yield strain (PYS) has clinical relevance as fractures are often regional in athletes (DeFranco et al., 2006). We hypothesize that age-related decline and variance in strength and PYS is not uniform throughout the male femora, but is driven by region-specific differences in porosity and composition. To test this hypothesis, we performed four-point bending tests on bone beams of anterior, posterior, medial, and lateral regions of the femoral midshaft, while porosity, ash content, and composition were analyzed from adjacent sections. Tissue-level mechanics, composition, and porosity between young and elderly men were compared. Multivariate regression models were used to identify trait(s) that best explained variance in strength and PYS for each region and after pooling data from all regions.

2. Materials and methods

2.1. Specimens

Cadaveric femora from 33 white male donors (18–89 yrs of age) were obtained through the University of Michigan Anatomical Donations Program (Ann Arbor, MI), Science Care (Phoenix, AZ), and Anatomy Gifts Registry (Hanover, MD). Males between 66 and 69 yrs of age were excluded to obtain a gap between young ($n = 20$, 18–63 yrs) and elderly ($n = 13$, 70–89 yrs) groups since elderly men ≥ 65 -yrs exhibit accelerated bone loss and increased fractures (Court-Brown and McQueen, 2016; Gielen et al., 2011; Szulc and Delmas, 2001). Donors had no known metabolic bone diseases. Right femora were cut to obtain 5 mm (proximal-to-midshaft) and 60 mm (distal-to-midshaft) thick-sections (Fig. 1). Tissue use was approved by the University of Michigan Institutional Biosafety Committee and declared exempt by the Institutional Review Board.

2.2. Four-point bending

Single rectangular beam (2.5 mm \times 5 mm \times 55 mm) was milled from each anterior, posterior, medial, and lateral quadrant (Fig. 1) using a customized computer-controlled mill. Beams were loaded to failure in four-point bending (Bigelow et al., 2019) whilst kept in a 37 °C bath of PBS with added calcium. Lower and lower span lengths were 42 mm and 18 mm, respectively. Load and deflection were converted to stress and strain using bending equations, taking yielding into consideration (Tommasini et al., 2005). Tissue-level strength (maximum stress) and post-yield strain (PYS, strain from yield-point to failure) were calculated from stress-strain curves (Jepsen et al., 2015). Fig. S3-4 show the

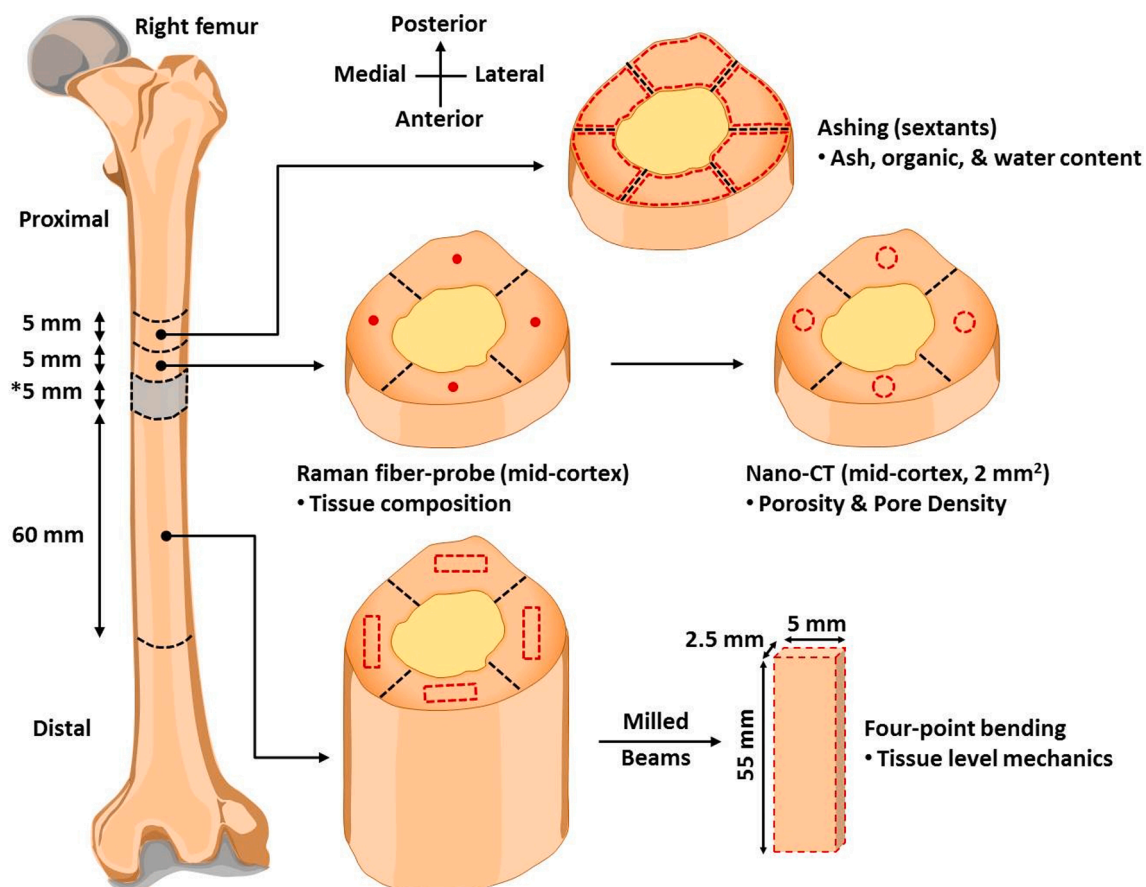


Fig. 1. Schematic illustrating the allocation of male femoral sections for ash and four-point bending tests and analysis by Raman spectroscopy and nanoCT. *Section not used in this study.

representative stress-strain curves for all four bone regions.

2.3. Ash content, Raman spectroscopy, and nanoCT

Ash, water, and organic content were measured (Bigelow et al., 2019; Tommasini et al., 2008). 5 mm-sections were analyzed using a Raman probe (Bigelow et al., 2019). Mid-cortical spectra were obtained under hydrated conditions using 6x10s acquisition times. Duplicate measurements were acquired from anterior, posterior, lateral, and medial regions (Fig. 1). Spectra were processed in MATLAB® and imported into GRAMS/AI™ for curve-fit analysis. Regional deconvoluted amide-I spectra can be found in Fig. S1-2. Select ratios were calculated: 960/1665 (mineral/matrix ratio, MMR), 875/853 (hydroxyproline/proline or Hyp/Pro), 1246/1269, 1665/1246, 1665/1691, and 1665/1631 cm^{-1} . 1665/1691 were used as measures of mature-trivalent to immature-divalent crosslinks (XLinks) (Mandair et al., 2021). Hyp/Pro is an indirect measure of post-translational modifications to collagen fibrils (Burke et al., 2016; Unal et al., 2018). 1246/1269 and 1665/1246 provide information on collagen orientation (Falgayrac et al., 2010; Mandair et al., 2021). 1665/1631 is a variant of 1670/1640, which measures amount of helical order in collagen (Unal et al., 2016). Mineral crystallinity (XLS) is inverse of $\nu_1\text{PO}_4$ bandwidth at $\sim 960 \text{ cm}^{-1}$. Our mean mid-cortical measurements reflect spectral contributions from both osteonal and interstitial features, but relative Raman property differences between osteonal and interstitial bone are presumed to be constant for a given specimen and parameter, and any deviations between young and elderly groups due to spatial differences within a group would be small.

After Raman analysis, 5 mm-sections were scanned by nanoCT. Each section was scanned at 13 μm voxel size (Bigelow et al., 2019; Bolger et al., 2020). Scans were reconstructed and regional porosity with 2- mm^2 ROIs examined (Fig. 1). Porosity was the total area of the pores divided by the area of the bone. Pore density was the number of pores divided by the area of the 2- mm^2 ROI.

2.4. Statistical analysis

Statistical analyses were performed in SPSS and results presented as mean \pm SDs. Normality was examined by Shapiro-Wilk tests in an age-specific manner. Porosity exhibited a non-normal distribution and was Logarithm-transformed. Adjusted (Adj.) R^2 -values, slopes, and y-intercepts of age-related linear regressions by bone region are reported, with significance set at $p < 0.05$. Age-specific differences in slopes of regression lines between regions were determined by ANCOVA (Bigelow et al., 2019). Holm-Bonferroni method was used for *post-hoc* statistical comparisons.

Independent-samples t-tests at the $p < 0.05$ level were used to compare donor age, weight, or height between young and elderly cohorts. Mixed-model statistics was used for side-by-side comparisons of traits between young and elderly cohorts by bone region. Repeated-measures ANOVA was used to compare trait differences between bone regions for each age group. For mix-model and repeated-measures ANOVA tests, significance was set at $p < 0.05$, which included Bonferroni corrections.

Age sensitivity analyses were performed where the size of the younger age group (18–63 yrs, $n = 20$) was incrementally reduced to one of the following: (1) 27–63 ($n = 18$), (2) 29–63 ($n = 16$), (3) 27–58 ($n = 13$), (4) 29–58 ($n = 11$), and (5) 18–45 ($n = 11$).

Multivariate regression analyses were performed to determine variance in strength or PYS, with variations in the independent traits for a given bone region and after pooling results across all regions (denoted by 'All' label). Systematic variable selection was used to identify 5-independent traits that explained variance in strength or PYS, they included: Log(porosity), MMR, XLS, Hyp/Pro, and 1246/1269. Backward selection was used to eliminate traits with $p > 0.05$ and variance inflation factor (VIF) ≥ 5 (Bigelow et al., 2019). Standardized β -coefficient values

for each of the independent traits used in the models are reported, together with accumulative model constant p -value, percent-adjusted R^2 (% Adj. R^2), regression p -value, and VIF.

3. Results

3.1. Donor characteristics and age-trait trajectory comparisons by bone region

Ages of young and elderly male cohorts were 43.0 ± 14.8 -yrs and 80.0 ± 6.3 -yrs, respectively (Table 1). Significant difference in age between young and elderly men ($p < 0.001$) was found, but not in weight ($p > 0.419$) or height ($p > 0.321$).

Representative nanoCT slices obtained from 35- and 78-yr old donors (Fig. 2A) show how porosity increased with age and bone region. Significant positive Log(porosity) vs. age regressions were found for anterior and posterior bones ($R^2 = 0.158$, $p = 0.013$ and $R^2 = 0.382$, $p < 0.001$, respectively), but not for lateral or medial bones ($R^2 = 0.031$, $p = 0.876$ and $R^2 = 0.014$, $p = 0.462$, respectively) (Fig. 2B, Table 2). Log (porosity) vs. age regressions between regions were significantly steeper in posterior than in medial or lateral bones ($p = 0.0071$ and $p = 0.0013$, respectively), while only significantly steeper in anterior than in lateral bone ($p = 0.0175$) (Table 3).

Significant negative regressions between strength and age were found for anterior, posterior, and lateral bones, but not for medial bone ($R^2 = 0.333$, $p = 0.001$; $R^2 = 0.360$, $p < 0.001$; $R^2 = 0.214$, $p = 0.009$; and $R^2 = 0.006$, $p = 0.368$, respectively) (Fig. 2C, Table 2). Strong negative regressions between post-yield strain and age were found for anterior and posterior bone ($R^2 = 0.362$, $p < 0.001$; $R^2 = 0.616$, $p < 0.001$), but not for lateral or medial bone ($R^2 = 0.047$, $p = 0.143$; and $R^2 = 0.079$ and $p = 0.076$; Fig. 2D, Table 2). Strength vs. age declined significantly faster anteriorly than medially ($p = 0.0050$, Table 3). While PYS vs. age declined faster anteriorly (Fig. 2D), it was not statistically significant ($p = 0.0386$, Table 3). All PYS measurements were in the range 0.01–0.025, which is consistent with other studies of cortical bone (Cowin, 2001). Although fractographic analyses were not performed, bones had observable post-yield displacement and did not fracture catastrophically upon yielding.

3.2. Age and regional differences in porosity and tissue-level mechanical properties

Significant increase in Log(porosity) was found in elderly compared to young men in posterior bone (Fig. 3A, $p < 0.05$). Posterior Log (porosity) was significantly higher than medial or lateral in both young and elderly men ($p < 0.001$ for all comparisons). In elderly men, anterior Log(porosity) was significantly higher than in lateral bone ($p = 0.028$). Posterior pore density was significantly lower than in medial bone in young men (Fig. 3B, $p = 0.018$). Strength was significantly higher in anterior bone of young vs. older men (Fig. 3C, $p < 0.05$), while PYS was significantly higher in anterior and posterior bones of young men (Fig. 3D, $p < 0.01$ for both). Strength did not vary across bone regions in young men, but anterior strength was significantly lower than medial and lateral strength in elderly men (Fig. 3C, $p = 0.001$ and $p = 0.021$,

Table 1
Age and anthropometric traits for young and elderly men.

Trait	Young (n = 20) Mean \pm S.D.	Elderly (n = 13) Mean \pm S.D.	p -value
Age Range (years)	18–63	70–89	–
Age (years)	43.0 ± 14.8	80.0 ± 6.3	< 0.001
Weight (kg)	90.6 ± 29.3	81.4 ± 18.7	0.419
Height (m)	1.78 ± 0.09	1.75 ± 0.07	0.321

Significant differences based on Independent-samples t -test ($p < 0.05$). Abbreviations: S.D., Standard Deviation.

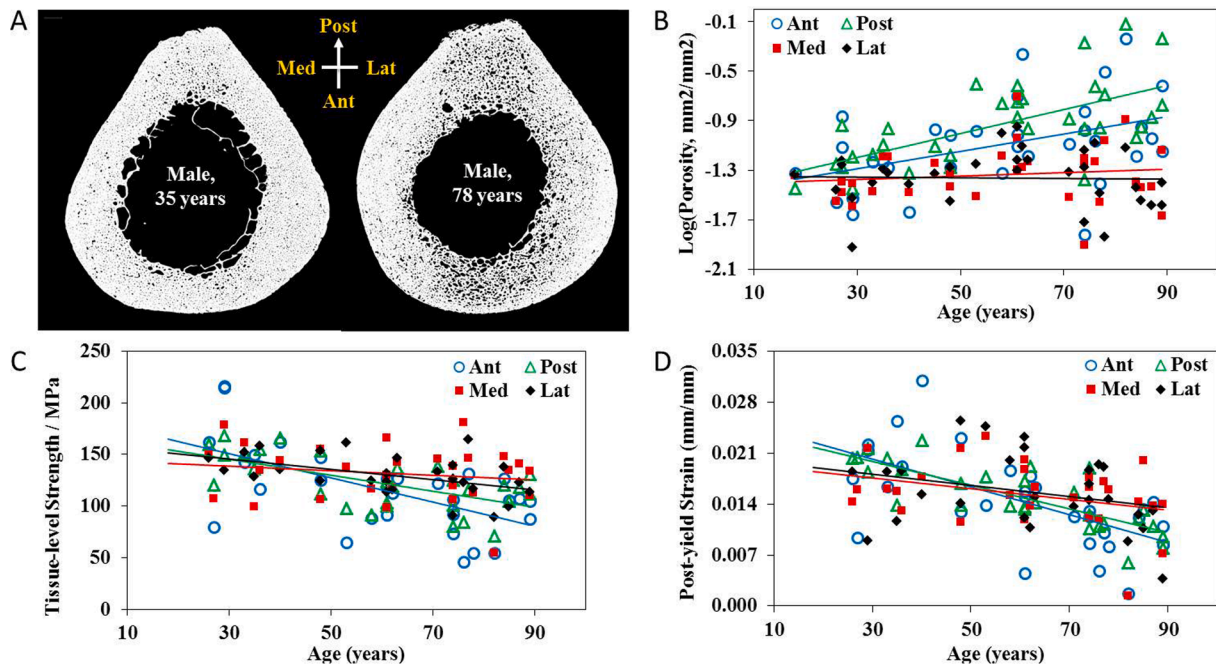


Fig. 2. (A) 2D transverse nanoCT slices of 35- and 78-year-old male femora with quadrantal landmarks (Ant = anterior, Lat = lateral, Post = posterior, Med = medial). Age-related linear regressions for (B) Log(porosity), (C) Tissue-level strength, and (D) Post-yield strain by bone quadrant. See Table 2 for linear regression Adj. R^2 values.

Table 2

Regression analysis showing the linear relationship between age and Log(porosity), Tissue-level strength, and Post-yield strain. **Notes:** Ant = anterior; Post = posterior; Lat = lateral; and Med = medial. Significant correlations are indicated in bold ($p < 0.05$).

Site	Age-Log(porosity)				Age-Tissue-level Strength				Age-Post-yield Strain			
	Adj R^2	y-Int	Slope	p-value	Adj R^2	y-Int	Slope	p-value	Adj R^2	y-Int	Slope	p-value
Ant	0.158	-1.500	0.007	0.013	0.333	186.5	-1.180	0.001	0.362	0.0259	-0.00019	<0.001
Post	0.382	-1.486	0.010	<0.001	0.360	168.6	-0.774	<0.001	0.616	0.0248	-0.00016	<0.001
Lat	0.031	-1.344	-0.000	0.876	0.214	161.1	-0.507	0.009	0.047	0.0205	-0.00008	0.143
Med	0.014	-1.415	0.001	0.462	0.006	145.8	-0.229	0.368	0.079	0.0198	-0.00007	0.076

Table 3

Age-trait slope comparisons between regressions of two bone quadrants (ANCOVA). The t -test and unadjusted p -values are listed, and bold indicates statistical significance according to the Holm-Bonferroni *post hoc* multiple comparison test.

Slopes Compared	Age-Log(porosity)		Age-Tissue Strength		Age-PYS	
	t-test	p-value	t-test	p-value	t-test	p-value
Med vs. Ant	1.8547	0.0660	-2.8691	0.0050	-2.0940	0.0386
Med vs. Post	2.7369	0.0071	-1.6338	0.1052	-1.6017	0.1122
Med vs. Lat	-0.5546	0.5802	-0.7812	0.4364	-0.0817	0.9351
Ant vs. Post	-0.8821	0.3794	1.2436	0.2164	-0.4894	0.6255
Ant vs. Lat	2.4093	0.0175	1.9320	0.0560	-1.9078	0.0591
Post vs. Lat	3.2914	0.0013	-0.4894	0.6255	-1.4412	0.1525

Notes: Ant = anterior; Post = posterior; Lat = lateral; Med = medial. See Fig. 2 and Table 3 for age-trait regressions by bone quadrant.

respectively). Significant slope age vs. trait differences between bone regions were found after incrementally narrowing the age range of the younger group (Table S1).

3.3. Age and regional differences in compositional traits

Ash content was significantly higher in elderly men compared to young men in posterior and medial bone (Fig. 4A, $p < 0.05$ or less). MMR

was significantly higher in elderly men in lateral bone (Fig. 4B). Ash content was significantly higher medially than anteriorly in both young and elderly men ($p = 0.036$ and $p = 0.003$, respectively), and higher posteriorly in elderly men ($p = 0.002$). Lateral ash content was higher than posterior and anterior bone in young and elderly men ($p < 0.001$ for both), while anterior ash content was higher than posterior bone in young men ($p < 0.001$). No significant differences were found in XLS (Fig. 4C).

Compared to elderly men, water content was significantly higher in young men in all regions (between $p < 0.01$ and $p < 0.05$, Fig. 5A). Anterior water content was significantly higher than in medial or lateral bones in young men ($p < 0.001$ and $p = 0.017$, respectively), but significantly lower than in posterior bone ($p < 0.001$). Posterior water content was significantly higher medially or laterally in young men ($p < 0.001$ and $p = 0.004$, respectively) and medially in elderly men ($p = 0.043$). Posterior Hyp/Pro was significantly higher in elderly men (Fig. 5B, $p < 0.01$) and anterior 1246/1269 was significantly higher in young men (Fig. 5C, $p < 0.05$). Posterior Hyp/Pro was significantly reduced compared to lateral bone in young men (Fig. 5B, $p = 0.037$) and anterior 1246/1269 was significantly higher than posterior bone in young men (Fig. 5C, $p = 0.013$). No significant differences were found in 1665/1691 (Fig. 5D) or 1665/1631 (Fig. S5A). A non-significant increase in 1665/1631 (Fig. S5B) was found across all bone regions in elderly men. From age sensitivity analyses, significant multiple trait differences between young and elderly groups by bone region were still found, and consistent with changes in the originally used cohort

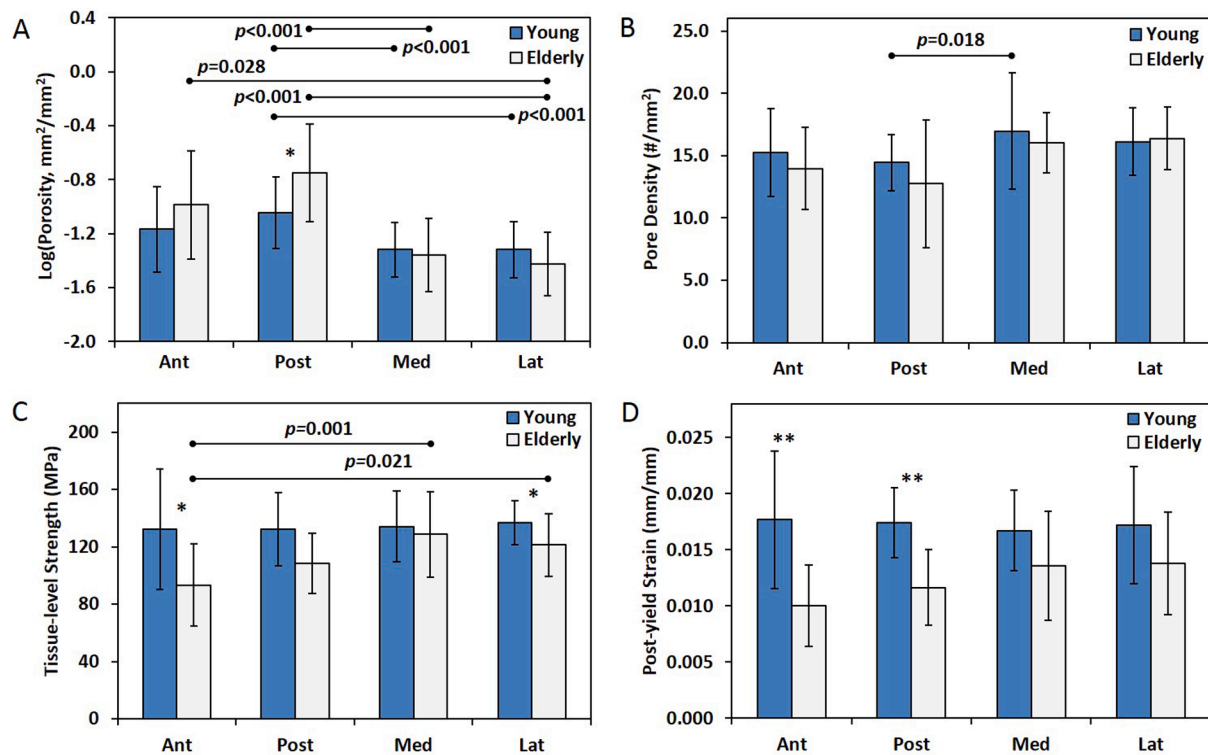


Fig. 3. Comparison of (A) Log(porosity), (B) Pore density, (C) Tissue-level strength, and (D) Post-yield strain between age groups and quadrant (Ant = anterior, Lat = lateral, Post = posterior, and Med = medial). Mixed-model age-related statistically significant differences were considered at the $p < 0.05$ (*) and $p < 0.01$ (**) levels. Connecting lines indicate regional differences with a significance threshold of $p < 0.05$. All statistical analyses include Bonferroni multiple comparison corrections.

(Table S2).

3.4. Predictors of tissue-level strength and PYS

Multivariate models were used to identify which 5-traits (Log (porosity), MMR, XLS, Hyp/Pro, and/or 1246/1269) contributed significantly to the prediction of strength and PYS by bone region. Significant predictors were judged by strength of β -coefficient(s) for each trait(s) used in the models, including overall strength of the % Adj. R^2 -value and $VIF < 2$. For strength, Log(porosity) + 1246/1269 explained 46.7% of the variance for anterior bone (Table 4, regression $p < 0.001$) compared to 50.5 and 13.1% by Log(porosity) for posterior and medial bones, respectively (regression $p < 0.001$ and $p = 0.036$, respectively). No traits significantly explained variance of strength for lateral bone (Table 4). For PYS, a combination of traits: (1) Log(porosity) + XLS + 1246/1269; (2) MMR + XLS + Hyp/Pro; or (3) MMR + Hyp/Pro + 1246/1269) significantly explained 46.3, 49.6, and 34.8% of variance for anterior, posterior, and lateral bones, respectively (Table 5, regression $p < 0.001$, $p < 0.001$, and $p = 0.005$, respectively). Hyp/Pro alone significantly explained 18.5% of variance of PYS for medial bone (regression $p = 0.011$). When locations were pooled, only Log(porosity) significantly explained 27.1 and 8.4% of variance in strength (Table 4) and PYS (Table 5), respectively (regression $p < 0.001$ and $p = 0.001$, respectively). Pore density, water content, collagen XLinks, 1665/1246, and 1665/1631 were not predictive of strength or PYS.

3.5. Discussion

Age-related increase in porosity and decline in tissue-level mechanical properties is not uniform throughout the human male femora. Greatest increase in porosity with age occurred in posterior and anterior bones (Fig. 2B, Table 2), and greatest decrease in strength and post-yield strain occurred in anterior bone (Fig. 2C-D, Table 2). Porosity and/or

certain aspects of composition explained 47–51% of variance in strength and PYS in the multivariate models of anterior and posterior bone (Tables 4 and 5) compared to 13% of variance in strength for medial bone and 19–35% of variance in PYS for medial and lateral bone. No traits adequately explained variance in strength for lateral bone.

Our findings of increased porosity and decreased strength and PYS in posterior and anterior bone with age (Figs. 2-3, Table 3) are consistent with an asymmetrical skeletal loading mechanism (Chan et al., 2007; Martin et al., 1998), where differential loading distribution across the femur may result in regional variations in remodeling and porosity. Lower differential loading along the anterior-posterior axis of the male femora may have contributed to the greater variation in porosity compared to the medial-lateral axis. Regional femoral differences have also been reported in adult sows, with anterior and posterior regions being more actively remodeled (Raab et al., 1991). In this study, age vs. Log(porosity) correlation values of $R^2 = 0.158$ determined for anterior bone (Table 2) were within the R^2 range of 0.135–0.461 reported in other studies (Bousson et al., 2001; Cooper et al., 2007). Strongest age vs. Log(porosity) correlation of $R^2 = 0.382$ was found for posterior bone (Table 2). This is the first age vs. Log(porosity) correlation reported for posterior bone.

Strength did not vary significantly between bone regions in men 18–65 yrs old (Fig. 3C). However, slope of the strength vs. age regression line for medial bone was significantly different from anterior bone (Fig. 2C, Table 3, $p < 0.005$) and values were lower for medial bone for ages < 45 -yrs. The trajectory was reversed above 45-yrs, with a steeper decline in strength in anterior bone with age compared to medial bone. Similar non-significant trend was also found for PYS vs. age regression lines between anterior and medial bones (Fig. 2D, Table 3, $p = 0.0386$). Reversal in age vs. strength and age vs. PYS trajectories between bone regions has not been reported before and may explain the higher incidences of medial and posteromedial femoral stress fractures reported in young athletes (DeFranco et al., 2006). It is believed that young

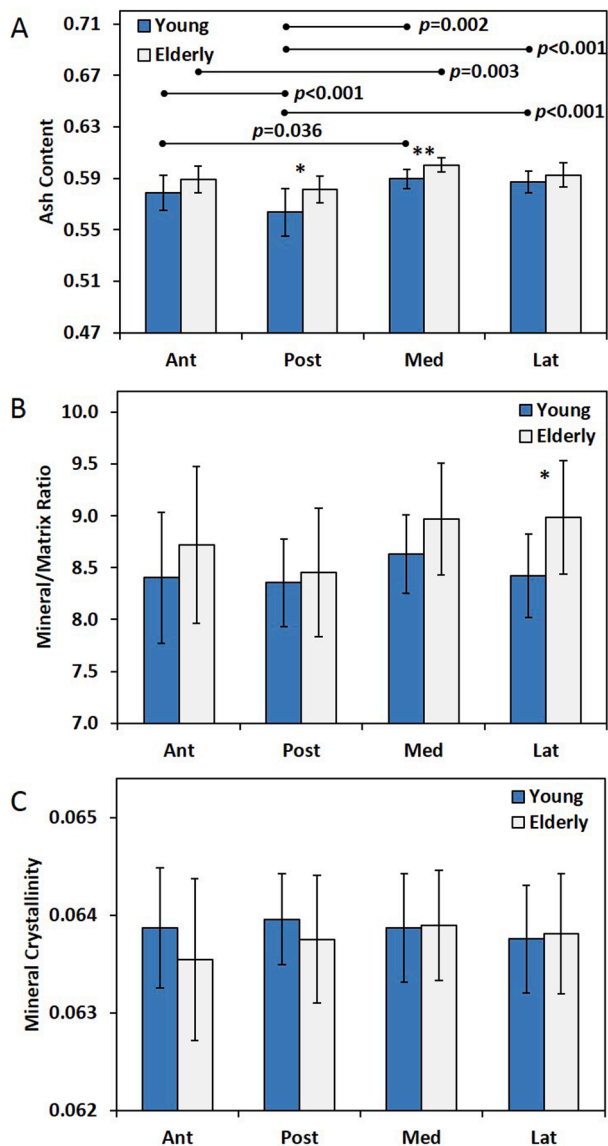


Fig. 4. Comparison of (A) Ash content, (B) Mineral/Matrix ratio, and (C) Mineral crystallinity between age groups and quadrant (Ant = anterior, Lat = lateral, Post = posterior, and Med = medial). Mixed-model age-related statistically significant differences were considered at the $p < 0.05$ (*) and $p < 0.01$ (**) levels. Connecting lines indicate regional differences with a significance threshold of $p < 0.05$. All statistical analyses include Bonferroni multiple comparison corrections.

athletes are at higher risk of fatigue-related stress fractures due to bone being subjected to repetitive loads over a short period of time (Abbott et al., 2020; Romani et al., 2002). Elderly men are susceptible to both fatigue and insufficiency fractures (Iundusi et al., 2013; Romani et al., 2002). Overall, regions with the highest porosity (e.g. posterior and anterior bones) in elderly men (Fig. 2B, 2A) experience the greatest negative impact on strength. This may explain why the trajectory of the age vs. strength regression line was steeper for anterior bone compared to medial bone at ages above 45-yrs (Fig. 2C).

Medial bone exhibited a significantly higher pore density compared to posterior bone in young men (Fig. 3B), which has not been observed before in human femora. One study showed that pore density was similar between bone regions at the femoral midshaft in men (Cooper et al., 2007), while the finding of posterior bone having the lowest pore density (Fig. 3B) is consistent with another study (Malo et al., 2013). Although, water content was higher in posterior bone than in anterior

bone in young men, the water content in both regions was significantly higher than in medial and lateral bones in young and elderly men (Fig. 5A). Decline in water content in elderly men (Fig. 5A) suggests that water bound to collagen and mineral is lost with age (Burr, 2019). Water content was inversely-related to ash content between regions and age groups (Fig. 5A, Fig. 4A). High ash content found in medial and posterior bones in elderly men was supported by similar trends in MMRs (Fig. 4B).

Despite the potential for increased heterogeneity introduced into our analyses by using a broader age range, significant slope age vs. Log (porosity), strength, or PYS differences between bone regions were still found (Table 3). Significant differences in multiple traits were also found between young (18–63 yrs) and elderly (70–89 yrs) age groups in spite of the greater perceived heterogeneity (Figs. 3–5). A 65-yr cutoff was used to define our two age groups because men ≥ 65 yrs of age exhibit accelerated bone loss and increased incidence of fractures (Court-Brown and McQueen, 2016; Gielen et al., 2011; Szulc and Delmas, 2001). In actuality, the cutoff in our study was 63-yrs, which is similar to other studies (Karasik et al., 2003; Singleton et al., 2021). Even after narrowing the age range of the young group of 18–63 yrs ($n = 20$, Table 1) to 29–58 or 18–45 yrs ($n = 11$, Table S1), significant slope age vs. trait differences between bone regions were still found. Reducing the size of the young age group did not affect multiple-trait differences between the two age groups (Tables S2–5). These age sensitivity analyses show that our primary findings and interpretations were not impacted by using a broader young group age range.

Raman 1246/1269 was significantly increased in anterior bone compared to posterior bone in young men (Fig. 5C). The 1246/1269 ratio is related to the relative orientation of collagen fibrils in bone (Mandair et al., 2021). High 1246/1269 ratios exhibited by anterior bone compared to posterior bone could be due to changes in relative distribution of longitudinally and transversely aligned collagen fibrils with age. This interpretation is supported by a light polarization study in which bone from young male femora contained collagen fibrils predominately orientated longitudinally as opposed to transversely in older males (Goldman et al., 2003).

No significant differences in collagen 1665/1691 (XLinks), 1665/1246 (orientation), or 1665/1631 (helical order) were found between bone regions or age groups (Fig. 5D, Fig. S5A, and Fig. S5B, respectively). Lack of significant regional differences in XLinks is consistent with an HPLC study, where mature-to-immature crosslink ratios were not significantly different between medial and lateral bones (Gauthier et al., 2018). In our earlier study (Bigelow et al., 2019), XLinks remained unchanged with age in narrow radii, but decreased in wide radii, suggesting that age-composition relations are not simple and can be mediated by other factors like external bone size (Bolger et al., 2020). This may account for the large standard deviations seen in some amide-I parameters (Fig. 5D and Fig. S5). We suspect that the amide-I component of 1665/1246 contains contributions from trivalent collagen crosslinks (Bart et al., 2014) and thus may explain why this parameter underperformed compared to 1246/1269 (Fig. 5C).

This study sought to identify independent traits that contributed to strength and post-yield in each bone region and to determine local mechanics-composition relations. From the strength of β -coefficients values (Tables 4–5), 1–3 independent traits related to Log(porosity), mineral crystallinity (XLS), mineral-to-matrix ratio (MMR), Hydroxyproline/Proline (Hyp/Pro), collagen crosslinks (XLinks) and 1246/1269 ratios made significant contributions to the multivariate models by bone region. For anterior bone, 47% of variance in strength and PYS was explained by Log(porosity) + 1246/1269, while Log(porosity) explained 51% of variance in strength in posterior bone. We posit that the prediction of strength and PYS by 1246/1269 is related to the observation that bone under tension (e.g. anterior bone), is more dependent on collagen orientation than bone under compression (e.g. posterior bone) (Meardon and Derrick, 2014; Ramasamy and Akkus, 2007).

Prediction of PYS in posterior bone was more complex, with 50% of

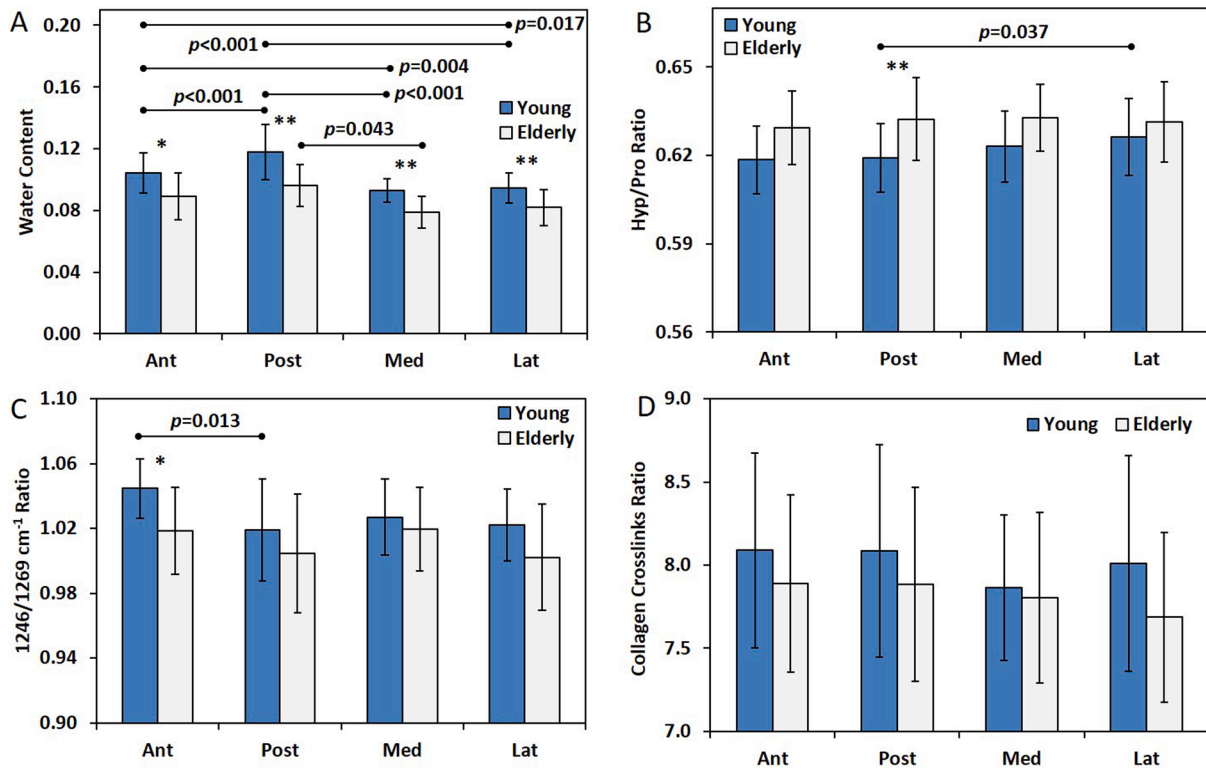


Fig. 5. Comparison of (A) Water content, (B) Hydroxyproline/Proline (Hyp/Pro) ratio (C) mature to immature cross-link ratio (1246/1269), and (D) Collagen crosslinks ratio between age groups and quadrant (Ant = anterior, Lat = lateral, Post = posterior, and Med = medial). Mixed-model age-related statistically significant differences were considered at the $p < 0.05$ (*) and $p < 0.01$ (**) levels. Connecting lines indicate regional differences with a significance threshold of $p < 0.05$. All statistical analyses include Bonferroni multiple comparison corrections.

Table 4

Multivariate regression models predicting tissue-level strength by bone region. Standardized β -coefficients shown for each trait(s). Accumulative Constant p , % Adj. R^2 , Regression p , and VIF values shown for each row.

Region	Standardized β -Coefficients					p -value (Constant)	% Adj. R^2	p -value (Regression)	Max VIF
	Log (Porosity)	MMR	XLS	Hyp/Pro	1246/1269				
Ant	-0.463	-	-	-	0.374	0.028	46.7	<0.001	1.227
Post	-0.723	-	-	-	-	<0.001	50.5	<0.001	-
Lat	-	-	-	-	-	-	-	-	-
Med	-0.405	-	-	-	-	<0.001	13.1	0.036	-
All	-0.527	-	-	-	-	<0.001	27.1	<0.001	-

Notes: Ant = anterior; Post = posterior; Lat = lateral; Med = medial; All = data pooled across all bone sites; Hyp/Pro = hydroxyproline/proline ratio; MMR = mineral/matrix ratio, XLS = mineral crystallinity, and VIF = variance inflation factor.

Table 5

Multivariate linear regression models predicting post-yield strain (PYS) by bone region. Standardized β -coefficients shown for each trait(s), Accumulative Constant p , % Adj. R^2 , Regression p , and VIF values shown for each row.

Region	Standardized β -Coefficients					p -value (Constant)	% Adj. R^2	p -value (Regression)	VIF
	Log (Porosity)	MMR	XLS	Hyp/Pro	1246/1269				
Ant	-0.375	-	0.320	-	0.414	0.004	46.3	<0.001	1.231
Post	-	-0.363	0.513	-0.581	-	0.320	49.6	<0.001	1.035
Lat	-	-0.670	-	-0.350	-0.595	0.002	34.8	0.005	1.490
Med	-	-	-	-0.463	-	0.004	18.5	0.011	-
All	-0.303	-	-	-	-	<0.001	8.4	0.001	-

Notes: Ant = anterior; Post = posterior; Lat = lateral; Med = medial; All = data pooled across all bone sites; Hyp/Pro = hydroxyproline/proline ratio; MMR = mineral/matrix ratio, XLS = mineral crystallinity, and VIF = variance inflation factor.

variance explained by XLS + MMR + Hyp/Pro. Only 35% of variance in PYS in lateral bone could be explained by MMR + Hyp/Pro + 1246/1269. Highly mineralized older bone permits only small post-yield deformation (Currey, 2004; Paschalis et al., 1997; Yerramshetty and Akkus, 2008). Lower PYS is consistent with the higher MMR and trend

toward lower PYS exhibited by lateral bone in elderly men (Fig. 4B, Fig. 3D). Basis for the low PYS exhibited by posterior bone in elderly men is unclear, as both XLS and MMR were similar between young and elderly men. Hyp/Pro also contributes to the variance in PYS in posterior, lateral, and medial bones, which indicates possible post-

translational modification of collagen (Mandair et al., 2021). Lack of traits that explain variance of strength in lateral bone is unclear, but suggests that lateral bone is less responsive to daily mechanical loads compared to other regions. This interpretation is based on a physical activity study, where tibial lateral and medial mass distributions were similar between active and non-active co-twins, while anterior and posterior mass distributions only increased in active co-twins (Ma et al., 2009).

Multivariate models of data pooled from all regions did not improve the prediction of strength or PYS (Tables 4-5), with only Log(porosity) persisting in the models. Given that porosity was a significant predictor in anterior and posterior multivariate models, inclusion of data from medial and lateral bones reduced the predictive power in the pooled model. Low variance explained by pooled models underscores the complexity of trait analysis of bone function. Variance not explained by our models may be attributed to traits not examined in this study (e.g. external bone size or muscle forces).

In conclusion, our study supports the hypothesis that age-related increases in porosity and declines in tissue-level strength and post-yield strain are region-specific, with the most pronounced decline found in anterior and posterior bones. This behavior is attributed to the non-uniform distribution of skeletal load across the midshaft. Consequently, prediction of bone mechanical properties varied, with porosity and/or traits related to composition explaining 46–51% of variance in strength and post-yield strain for anterior and posterior bone compared to 0–35% for lateral and 13–19% for medial bone. Predictive performance of our multivariate models was negatively impacted by pooling data from all bone regions, which underscores the complexity of the femur and that pooled analyses may obscure underlying region-specific differences. A combined approach of region and pooled analyses may provide a more complete assessment of the complex relationship between tissue mechanics, porosity, and composition. Results of this study may have implications in the clinical prediction or prevention of regional femoral stress fractures in young athletes.

CRedit authorship contribution statement

Gurjit S. Mandair: Writing – original draft, Writing – review & editing, Methodology, Formal analysis, Data curation, Conceptualization. **Erin M.R. Bigelow:** Writing – review & editing, Methodology, Formal analysis, Data curation, Conceptualization. **Gowri Viswanathan:** Writing – review & editing, Formal analysis, Data curation. **Ferrous S. Ward:** Writing – review & editing, Data curation. **Daniella M. Patton:** Writing – review & editing, Data curation. **Stephen H. Schlecht:** Writing – review & editing, Data curation. **Karl J. Jepsen:** Writing – review & editing, Supervision, Resources, Funding acquisition, Conceptualization. **David H. Kohn:** Writing – review & editing, Supervision, Resources, Funding acquisition, Conceptualization.

Declaration of Competing Interest

The authors declare that they have no known competing financial interests or personal relationships that could have appeared to influence the work reported in this paper.

Acknowledgements

Study was supported by the National Institute of Arthritis and Musculoskeletal and Skin Diseases of the National Institutes of Health (KJJ: AR065424, AR069620, AR068452; SHS: AR070903; DHK. MWB: T32DE007057). Authors thank Dr. Christopher Robbins (University of Michigan) and Center for Statistical Consultation and Research (University of Michigan) for statistical advice. Authors thank Dr. Michael Morris (University of Michigan) and Morgan Bolger (University of Michigan) for discussions and feedback. Authors' roles: Study design and conception: KJJ, DHK, EMR, GSM. Data collection: EMR, DMP, FSW, GSM. Statistical analysis: GSM, GV, EMR. Data interpretation: All

authors. Writing - manuscript draft: GSM, EMR. Writing - revisions: All authors. Data integrity: GSM, EMR, KJJ, DHK.

Appendix A. Supplementary material

Supplementary data to this article can be found online at <https://doi.org/10.1016/j.jbiomech.2022.111144>.

References

- Abbott, A., Bird, M., Brown, S.M., Wild, E., Stewart, G., Mulcahey, M.K., 2020. Part II: presentation, diagnosis, classification, treatment, and prevention of stress fractures in female athletes. *Phys. Sportsmed.* 48 (1), 25–32.
- Bart, Z.R., Hammond, M.A., Wallace, J.M., 2014. Multi-scale analysis of bone chemistry, morphology and mechanics in the oim model of osteogenesis imperfecta. *Connect. Tissue Res.* 55 (sup1), 4–8.
- Bell, K.L., Loveridge, N., Reeve, J., Thomas, C.D.L., Feik, S.A., Clement, J.G., 2001. Super-osteons (remodeling clusters) in the cortex of the femoral shaft: Influence of age and gender. *Anat. Rec.* 264 (4), 378–386.
- Bigelow, E.M.R., Patton, D.M., Ward, F.S., Ciarelli, A., Casden, M., Clark, A., Goulet, R.W., Morris, M.D., Schlecht, S.H., Mandair, G.S., Bredbenner, T.L., Kohn, D.H., Jepsen, K.J., 2019. External bone size is a key determinant of strength-decline trajectories of aging male radii. *J. Bone Miner. Res.* 34 (5), 825–837.
- Bolger, M.W., Romanowicz, G.E., Bigelow, E.M.R., Ward, F.S., Ciarelli, A., Jepsen, K.J., Kohn, D.H., 2020. External bone size identifies different strength-decline trajectories for the male human femora. *J. Struct. Biol.* 212 (3), 107650.
- Bousson, V., Meunier, A., Bergot, C., Vicaut, É., Rocha, M.A., Morais, M.H., Laval-Jeantet, A.-M., Laredo, J.-D., 2001. Distribution of intracortical porosity in human midfemoral cortex by age and gender. *J. Bone Miner. Res.* 16 (7), 1308–1317.
- Burke, M.V., Atkins, A., Akens, M., Willett, T.L., Whyne, C.M., 2016. Osteolytic and mixed cancer metastasis modulates collagen and mineral parameters within rat vertebral bone matrix. *J. Orthop. Res.* 34 (12), 2126–2136.
- Burr, D.B., 2019. Changes in bone matrix properties with aging. *Bone* 120, 85–93.
- Burstein, A.H., Reilly, D.T., Martens, M., 1976. Aging of bone tissue: mechanical properties. *J. Bone Joint Surg. Am.* 58 (1), 82–86.
- Chan, A.H.W., Crowder, C.M., Rogers, T.L., 2007. Variation in cortical bone histology within the human femur and its impact on estimating age at death. *Am. J. Phys. Anthropol.* 132 (1), 80–88.
- Choksi, P., Jepsen, K.J., Clines, G.A., 2018. The challenges of diagnosing osteoporosis and the limitations of currently available tools. *Clin. Diabetes Endocrinol.* 4, 12.
- Cooper, D.M.L., Thomas, C.D.L., Clement, J.G., Turinsky, A.L., Sensen, C.W., Hallgrímsson, B., 2007. Age-dependent change in the 3D structure of cortical porosity at the human femoral midshaft. *Bone* 40 (4), 957–965.
- Court-Brown, C.M., McQueen, M.M., 2016. Global Forum: Fractures in the Elderly. *J. Bone Joint Surg.-Am.* 98 (9), e36.
- Cowin, S.C., 2001. *Bone mechanics handbook*. CRC Press, Boca Raton, FL.
- Currey, J.D., 2004. Tensile yield in compact bone is determined by strain, post-yield behaviour by mineral content. *J. Biomech.* 37 (4), 549–556.
- DeFranco, M.J., Recht, M., Schils, J., Parker, R.D., 2006. Stress fractures of the femur in athletes. *Clin. Sports Med.* 25 (1), 89–103.
- Falgayrac, G., Facq, S., Leroy, G., Cortet, B., Penel, G., 2010. New method for Raman investigation of the orientation of collagen fibrils and crystallites in the Haversian system of bone. *Appl. Spectrosc.* 64 (7), 775–780.
- Gauthier, R., Follet, H., Langer, M., Gineyts, E., Rongieras, F., Peyrin, F., Mitton, D., 2018. Relationships between human cortical bone toughness and collagen cross-links on paired anatomical locations. *Bone* 112, 202–211.
- Gielen, E., Vanderschueren, D., Callewaert, F., Boonen, S., 2011. Osteoporosis in men. *Best Pract. Res. Clin. Endoc. Metab.* 25 (2), 321–335.
- Goldman, H.M., Bromage, T.G., Thomas, C.D.L., Clement, J.G., 2003. Preferred collagen fiber orientation in the human mid-shaft femur. *Anat. Rec. A Discov. Mol. Cell. Evol. Biol.* 272A, 434–445.
- Goldman, H.M., Hampson, N.A., Guth, J.J., Lin, D., Jepsen, K.J., 2014. Intracortical remodeling parameters are associated with measures of bone robustness. *Anat. Rec. (Hoboken)* 297 (10), 1817–1828.
- Granke, M., Makowski, A.J., Uppuganti, S., Nyman, J.S., 2016. Prevalent role of porosity and osteonal area over mineralization heterogeneity in the fracture toughness of human cortical bone. *J. Biomech.* 49 (13), 2748–2755.
- Iundusi, R., Scialdoni, A., Arduini, M., Battisti, D., Piperno, A., Gasbarra, E., Tarantino, U., 2013. Stress fractures in the elderly: different pathological features compared with young patients. *Aging Clin. Exp. Res.* 25 (S1), 89–91.
- Jepsen, K.J., Centi, A., Duarte, G.F., Galloway, K., Goldman, H., Hampson, N., Lappe, J. M., Cullen, D.M., Greeves, J., Izard, R., Nindl, B.C., Kraemer, W.J., Negus, C.H., Evans, R.K., 2011. Biological constraints that limit compensation of a common skeletal trait variant lead to inequivalence of tibial function among healthy young adults. *J. Bone Miner. Res.* 26 (12), 2872–2885.
- Jepsen, K.J., Silva, M.J., Vashishth, D., Guo, X.E., van der Meulen, M.CH., 2015. Establishing Biomechanical mechanisms in mouse models: Practical guidelines for systematically evaluating phenotypic changes in the diaphyses of long bones. *J. Bone Miner. Res.* 30 (6), 951–966.
- Karasik, D., Cupples, L.A., Hannan, M.T., Kiel, D.P., 2003. Age, gender, and body mass effects on quantitative trait loci for bone mineral density: the Framingham Study. *Bone* 33 (3), 308–316.

- Ma, H., Leskinen, T., Alen, M., Cheng, S., Sipilä, S., Heinonen, A., Kaprio, J., Suominen, H., Kujala, U.M., 2009. Long-term leisure time physical activity and properties of bone: A twin study. *J. Bone Miner. Res.* 24 (8), 1427–1433.
- Malo, M.K.H., Rohrbach, D., Isaksson, H., Töyräs, J., Jurvelin, J.S., Tamminen, I.S., Kröger, H., Raum, K., 2013. Longitudinal elastic properties and porosity of cortical bone tissue vary with age in human proximal femur. *Bone* 53 (2), 451–458.
- Mandair, G.S., Akhter, M.P., Esmonde-White, F.W.L., Lappe, J.M., Bare, S.P., Lloyd, W.R., Long, J.P., Lopez, J., Kozloff, K.M., Recker, R.R., Morris, M.D., 2021. Altered collagen chemical compositional structure in osteopenic women with past fractures: A case-control Raman spectroscopic study. *Bone* 148, 115962.
- Martin, R.B., Burr, D.B., Sharkey, N.A., 1998. *Skeletal Tissue Mechanics*. Springer, New York.
- McCalden, R.W., McGeough, J.A., Barker, M.B., Court-Brown, C.M., 1993. Age-related changes in the tensile properties of cortical bone. The relative importance of changes in porosity, mineralization, and microstructure. *J. Bone Joint Sur. Am.* 75 (8), 1193–1205.
- Meardon, S.A., Derrick, T.R., 2014. Effect of step width manipulation on tibial stress during running. *J. Biomech.* 47 (11), 2738–2744.
- Norman, T.L., Wang, Z., 1997. Microdamage of human cortical bone: Incidence and morphology in long bones. *Bone* 20 (4), 375–379.
- Paschalis, E.P., Betts, F., DiCarlo, E., Mendelsohn, R., Boskey, A.L., 1997. FTIR microspectroscopic analysis of human iliac crest biopsies from untreated osteoporotic bone. *Calcif. Tissue Int.* 61 (6), 487–492.
- Raab, D.M., Crenshaw, T.D., Kimmel, D.B., Smith, E.L., 1991. A histomorphometric study of cortical bone activity during increased weight-bearing exercise. *J. Bone Miner. Res.* 6 (7), 741–749.
- Ramasamy, J.G., Akkus, O., 2007. Local variations in the micromechanical properties of mouse femur: The involvement of collagen fiber orientation and mineralization. *J. Biomech.* 40 (4), 910–918.
- Ramchand, S.K., Seeman, E., 2018. The influence of cortical porosity on the strength of bone during growth and advancing age. *Curr. Osteoporos. Rep.* 16 (5), 561–572.
- Reilly, G.C., Currey, J.D., 1999. The development of microcracking and failure in bone depends on the loading mode to which it is adapted. *J. Exp. Biol.* 202 (Pt 5), 543–552.
- Rizzoli, R., Bianchi, M.L., Garabédian, M., McKay, H.A., Moreno, L.A., 2010. Maximizing bone mineral mass gain during growth for the prevention of fractures in the adolescents and the elderly. *Bone* 46 (2), 294–305.
- Romani, W.A., Gieck, J.H., Perrin, D.H., Saliba, E.N., Kahler, D.M., 2002. Mechanisms and management of stress fractures in physically active persons. *J. Athl. Train.* 37, 306–314.
- Ruff, C., Holt, B., Trinkaus, E., 2006. Who's afraid of the big bad wolf? "Wolf is law" and bone functional adaptation. *Am. J. Phys. Anthropol.* 129, 484–498.
- Schlecht, S.H., Pinto, D.C., Agnew, A.M., Stout, S.D., 2012. Brief communication: The effects of disuse on the mechanical properties of bone: What unloading tells us about the adaptive nature of skeletal tissue. *Am. J. Phys. Anthropol.* 149 (4), 599–605.
- Singleton, R.C., Pharr, G.M., Nyman, J.S., 2021. Increased tissue-level storage modulus and hardness with age in male cortical bone and its association with decreased fracture toughness*. *Bone* 148.
- Skedros, J.G., Keenan, K.E., Williams, T.J., Kiser, C.J., 2013. Secondary osteon size and collagen/lamellar organization ("osteon morphotypes") are not coupled, but potentially adapt independently for local strain mode or magnitude. *J. Struct. Biol.* 181, 95–107.
- Szulc, P., Delmas, P.D., 2001. Biochemical markers of bone turnover in men. *Calcif. Tissue Int.* 69, 229–234.
- Thomas, C.D.L., Feik, S.A., Clement, J.G., 2005. Regional variation of intracortical porosity in the midshaft of the human femur: age and sex differences. *J. Anat.* 206, 115–125.
- Tommasini, S.M., Nasser, P., Hu, B., Jepsen, K.J., 2008. Biological co-adaptation of morphological and composition traits contributes to mechanical functionality and skeletal fragility. *J. Bone Miner. Res.* 23, 236–246.
- Tommasini, S.M., Nasser, P., Schaffler, M.B., Jepsen, K.J., 2005. Relationship between bone morphology and bone quality in male tibias: Implications for stress fracture risk. *J. Bone Miner. Res.* 20, 1372–1380.
- Turner, C.H., 2002. Biomechanics of bone: Determinants of skeletal fragility and bone quality. *Osteoporosis Int.* 13, 97–104.
- Unal, M., Jung, H., Akkus, O., 2016. Novel Raman spectroscopic biomarkers indicate that postyield damage denatures bone's collagen. *J. Bone Miner. Res.* 31, 1015–1025.
- Unal, M., Uppuganti, S., Leverant, C.J., Creecy, A., Granke, M., Voziyan, P., Nyman, J.S., 2018. Assessing glycation-mediated changes in human cortical bone with Raman spectroscopy. *J. Biophotonics* 11, 15.
- van Oers, R.F.M., Ruimerman, R., van Rietbergen, B., Hilbers, P.A.J., Huiskes, R., 2008. Relating osteon diameter to strain. *Bone* 43, 476–482.
- Yeni, Y.N., Brown, C.U., Wang, Z., Norman, T.L., 1997. The influence of bone morphology on fracture toughness of the human femur and tibia. *Bone* 21, 453–459.
- Yerramshetty, J.S., Akkus, O., 2008. The associations between mineral crystallinity and the mechanical properties of human cortical bone. *Bone* 42, 476–482.
- Yerramshetty, J.S., Lind, C., Akkus, O., 2006. The compositional and physicochemical homogeneity of male femoral cortex increases after the sixth decade. *Bone* 39, 1236–1243.
- Zebaze, R., Atkinson, E.J., Peng, Y., Bui, M., Ghasem-Zadeh, A., Khosla, S., Seeman, E., 2019. Increased cortical porosity and reduced trabecular density are not necessarily synonymous with bone loss and microstructural deterioration. *JBMR Plus* 3, e10078.